Theory of spin-polarized transport in photoexcited semiconductor/ferromagnet tunnel junctions

R. Jansen,* M. W. J. Prins,† and H. van Kempen
Research Institute for Materials, University of Nijmegen, Toernooiveld 1, 6525 ED Nijmegen, The Netherlands
(Received 23 July 1997)

We present a theory for spin-polarized transport in tunnel junctions consisting of a ferromagnet and a semiconductor, in which spin-polarized carriers are created by optical orientation. The model includes, for both spin orientations, the current due to tunneling between the ferromagnet and the semiconductor surface as well as the photoinduced and the thermionic emission currents through the semiconductor subsurface region. Tunneling is described in terms of a spin-dependent tunnel conductance, taking account of the magnetic structure of the ferromagnet. We consider spin depolarization of photoexcited electrons in the semiconductor bulk material and in surface states that have a spin-dependent occupation. The total tunnel current is evaluated as well as current modulations due to modulated spin polarization of photoelectrons (CPM signal) or modulated optical intensity. The calculations show that the CPM signal is proportional to the tunnel conductance polarization and is relatively insensitive to spin depolarization of photoelectrons during their transport to the surface. A severe signal reduction can, however, result from spin relaxation in semiconductor surface states. In addition, it is demonstrated that a crucial role is played by the operating regime of the junction, i.e., photoamperic or photovoltaic, where the selection is determined mainly by the choice of applied bias voltage. We find that the photovoltaic mode is favored, as it yields the highest contribution from spin-polarized tunneling, combined with the smallest sensitivity for unwanted light intensity modulations. [S0163-1829(98)03207-X]

I. INTRODUCTION

For a number of decades it has been known that spin-polarized carriers can be generated in semiconductors by optical means. This so-called optical orientation[1] of electrons is used mainly in spin-polarized electron sources,[2,3] developed during the late 1970s. Optical spin orientation can be achieved in most III-V semiconductor materials due to the presence of a sizable spin-orbit interaction. This causes the valence-band degeneracy near the center of the Brillouin zone to be partially lifted such that spin-polarized excess electrons are created upon illumination with circularly polarized light. In theory the polarization is 50% for GaAs at excitation resonant with the band gap and values approaching this have been measured in experiment.[2,3]

Shortly after the invention of the scanning tunneling microscope (STM), the use of III-V semiconductors and optical orientation was proposed as a possible way of obtaining spin sensitivity in STM.[4,5] The basic idea is to optically excite spin-polarized carriers in a semiconductor STM tip and thereby create a spin-dependent occupation of the energy levels. The tunnel current between such a tip and a magnetic sample will depend on the electron polarization in both the tip and sample and can thus be used to probe the spin-dependent electronic properties of the sample.

The application of this technique in a tunneling junction has been demonstrated recently using planar $Co/Al_2O_3/GaAs$ devices.[6,7] For the STM geometry, a number of experiments supporting the feasibility of the method have been conducted.[8,9] Theoretical descriptions of spin-polarized transport in ferromagnet/semiconductor junctions also have been given.[10–12] These treatments focus on the tunneling process itself, while charge flows inside the semiconductor were ignored. However, in a recent paper[13] on the photoelectrical properties of these tunnel junctions, we have shown that currents in the semiconductor cannot be neglected and may even dominate the transport behavior of the junction. We therefore have to address the question what influence the subsurface currents in the semiconductor have on the spin polarization of the tunnel current. This is the topic of the present paper, in which we extend our model of Ref. 13 by including the spin variable.[14]

Hence we will describe a fully spin-polarized theory for transport in photoexcited semiconductor/ferromagnet tunnel junctions that includes tunneling as well as the semiconductor subsurface currents. Moreover, spin relaxation in the semiconductor bulk and at the surface is considered. The model is used to calculate charge flows under optical orientation in order to elucidate the mechanisms that control the size of polarization signals and investigate the influence of several variables. In particular, we show that modulating the polarization of optically excited electrons creates an oscillation of the tunnel current that depends critically on the operating regime of the junction. The latter is determined mainly by the applied bias voltage. In addition, it is revealed that a significant signal reduction can arise from spin relaxation of photoelectrons in semiconductor surface states. The insight gained is indispensable for the interpretation of experimental results and valuable for the guidance of future work.

The paper is outlined as follows. In Sec. II the spin-polarized transport theory is presented. This is used to calculate the magnitude of spin-polarized tunneling signals in Sec. III. There we also describe the functional dependence on bias voltage, size and polarization of tunnel conductance, illumination intensity, and the spin-relaxation time in semiconductor bulk and at the surface. Simultaneously we obtain the optical response of the junction. The results are discussed in Sec. IV and Sec. V contains a summary and concluding remarks.

II. MODEL DESCRIPTION

In this section we introduce the model developed for spin-polarized transport in a tunnel junction between a ferromagnet and a semiconductor, in which spin-polarized carriers are created by optical spin orientation. We will limit the discussion to semiconductors of p-type doping and use parameters for GaAs throughout the paper. First we describe the spin polarization of the tunnel current. Then we consider the currents in the semiconductor subsurface region and include spin relaxation in the bulk as well as at the semiconductor surface. For one particular regime, an approximate analytical expression will be derived for the oscillation in the tunnel current due to modulated optical orientation.

A. Spin-polarized tunneling

We describe tunneling using the transfer Hamiltonian approach, which is a first-order perturbation method valid for the case of low tunnel barrier transparency. For the surface of the ferromagnetic electrode we define spin-dependent densities of states by ρ_m^σ and an energy distribution function F_m independent of spin. The superscript σ denotes the spin orientation with respect to a given quantization axis (either parallel $\uparrow$ or antiparallel $\downarrow$). For the (nonmagnetic) semiconductor the density of states ρ_s does not depend on spin. However, optical orientation produces an energy distribution F_s^σ at the semiconductor surface, which is different for the two spin directions.

When no scattering centers are present in the tunnel barrier, the electron energy ε and spin are conserved during the process of tunneling. The tunnel current (I_t^σ) for spin orientation σ from the magnetic material to the semiconductor is then expressed as

$$I_t^\sigma = \frac{-1}{e}\int d\varepsilon [F_m(\varepsilon + eV_m) - F_s^\sigma(\varepsilon)] G_t^\sigma(\varepsilon), \qquad (1)$$

$$G_t^\sigma(\varepsilon) = \frac{2\pi e^2}{\hbar} |M^\sigma(\varepsilon)|^2 \rho_s(\varepsilon) \rho_m^\sigma(\varepsilon + eV_m), \qquad (2)$$

where e is the absolute magnitude of the electron charge. The magnetic electrode is at the externally applied potential V_m, while the zero energy is given by the Fermi level in the semiconductor bulk. The function G_t^σ contains the densities of states and $M^\sigma(\varepsilon)$, an energy-dependent tunneling matrix element[16] that takes account of the overlap of the wave functions of the respective electrode materials. In the case of a magnetic material, not only ρ_m^σ, but also the matrix element is spin-dependent because the wave functions depend on spin. The tunnel current polarization, defined as $(I_t^\uparrow - I_t^\downarrow)/(I_t^\uparrow + I_t^\downarrow)$, is determined by the difference between $G_t^\uparrow$ and $G_t^\downarrow$, together with the spin imbalance in the semiconductor ($F_s^\uparrow \neq F_s^\downarrow$).

So far, no approximations have been made regarding the energy dependence of the densities of states and the matrix elements. Also the distribution functions F have not been specified yet. With respect to the latter, we presume that at the semiconductor surface each spin subsystem is in thermal equilibrium. This is a reasonable assumption considering the effectiveness of carrier capture and relaxation at semiconductor surfaces with surface states.[19] For each spin subsystem we can then properly assign a surface electrochemical potential V_s^σ and the electron distribution is given by an energy-shifted Fermi-Dirac function, i.e., $F_s^\sigma(\varepsilon) \simeq f(\varepsilon + eV_s^\sigma)$. As a further simplification, we will consider the regime of low temperature and low bias voltages. In this limit the current is linear in the bias voltage[20] and Eq. (1) reduces to

$$I_t^\sigma = G_t^\sigma [V_m - V_s^\sigma]. \qquad (3)$$

Note that the function G_t^σ effectively behaves as a tunnel conductance. In our model, we will treat G_t as a spin-dependent constant and disregard any deviations from a linear bias dependence.

In an experiment it is convenient to modulate the circular polarization of the excitation light and thereby the spin polarization of the created carriers. Using time-dependent surface potentials $V_s^\sigma(t) = \mathrm{Re}\{V_s^\sigma + \Delta V_s^\sigma \exp(j\omega t)\}$, we can calculate the resulting modulation of the total tunnel current. This yields

$$\Delta I_t = -\{ \underbrace{[G_t^\uparrow + G_t^\downarrow]\,\Delta\overline{V_s}}_{\text{spin-integrated}} + \underbrace{[G_t^\uparrow - G_t^\downarrow]\,\Delta V_s^{\text{spin}}}_{\text{spin-selective}} \}, \qquad (4)$$

where $\Delta\overline{V_s} = [\Delta V_s^\uparrow + \Delta V_s^\downarrow]/2$ and $\Delta V_s^{\text{spin}} = [\Delta V_s^\uparrow - \Delta V_s^\downarrow]/2$. Equation (4) shows that for modulated optical orientation ($\Delta V_s^\uparrow \neq 0$ and $\Delta V_s^\downarrow \neq 0$), the tunnel current modulation will in principle depend on the magnetic structure of the sample electrode via the function G_t^σ. More precisely, the modulation will change its phase by 180° upon reversal of the sample magnetization[21] (corresponding to interchanging $G_t^\uparrow$ and $G_t^\downarrow$) and has a size determined by the degree of tunnel conductance polarization (i.e., by $G_t^\uparrow - G_t^\downarrow$). The current modulation therefore reflects the magnetic structure of the sample.

As already stated, $G_t^\sigma(\varepsilon)$ contains the spin-dependent density of states in the magnetic electrode and a transition matrix element. It is therefore important to realize that, strictly speaking, one is sensitive not only to the spin polarization of the magnetic electrode, but also to the spin-dependent decay of the wave function into the tunnel barrier. Using free-electron states, it was already shown that the current polarization is affected by the height and shape of the tunneling barrier.[11,12] Furthermore, we stress that the tunnel current polarization is determined by those states that are contributing to the current. These are generally located in a narrow energy range around the Fermi level, while states with s- or p-character may dominate over d-type states, which are more localized in nature. To what extent the polarization of the tunnel current reflects the band polarization or the magnetic moments of the magnetic electrode is unclear at present.

B. Semiconductor subsurface currents

Transport in a tunnel junction between a metal and an optically excited semiconductor is quite complicated because, in addition to the actual tunneling current, also the electron and hole currents in the subsurface region of the semiconductor have to be included. Together these determine the (spin-dependent) occupation of the semiconductor

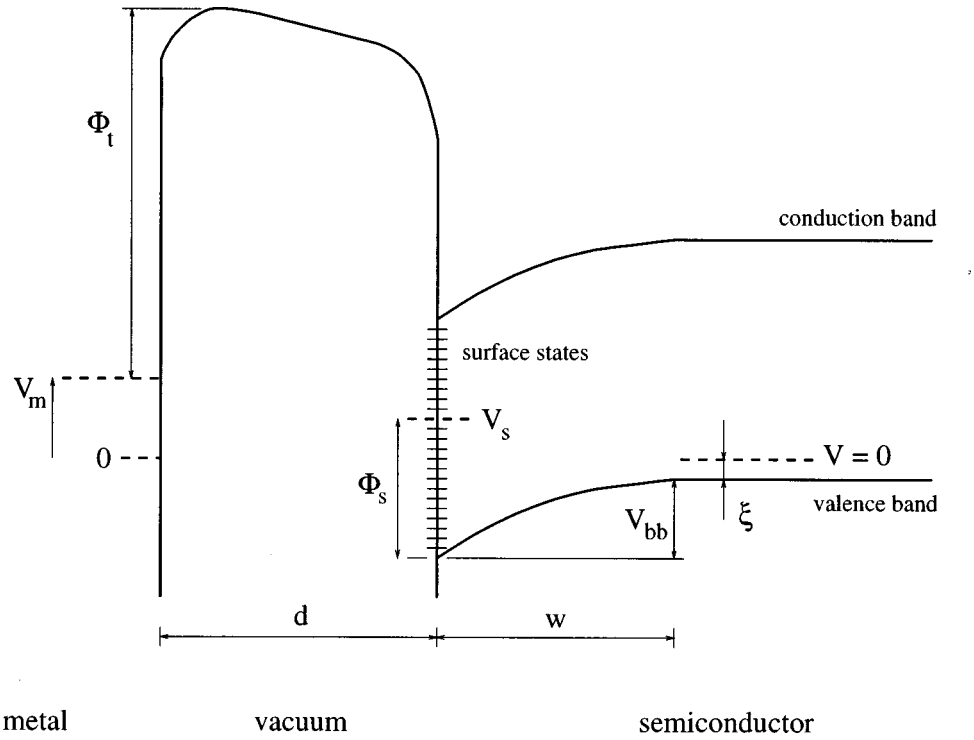

FIG. 1. Energy band diagram of a junction between a metal and a p-type semiconductor separated by a tunnel barrier of width d and height Φ_t. The zero potential is taken at the Fermi level in the semiconductor bulk, while the semiconductor surface and the metal electrode are at potentials V_s and V_m, respectively (both negative for the case shown). Also indicated are the width w of the depletion region, the amount of band bending V_{bb}, the Schottky barrier height Φ_s, and a parameter ξ as defined in the text.

surface states and thereby the tunnel current polarization [see Eq. (1)]. In the following we will describe the semiconductor subsurface currents as well as spin relaxation in surface states. For simplicity, tunnel junctions with *planar symmetry* are considered, although in our experiments we are dealing with low-symmetry STM junctions.[15,22] The description is based on the nonpolarized transport model that was discussed in a previous paper,[13] in which also the influence of the STM geometry, the calculation of time-dependent signals, and a comparison with experimental results was given.

In a tunnel junction between a semiconductor and a metal, generally a space-charge layer is present in the semiconductor subsurface region. The phenomenon can result from work function differences and/or the formation of surface/interface states and may be influenced by application of a bias voltage over the junction. For most p-type semiconductors, the subsurface region is depleted of holes and it can act as a barrier for transport. This so-called Schottky barrier is responsible for the well-known rectifying behavior of metal-insulator-semiconductor diodes.

For our transport model, we thus have to deal with a serial arrangement of a tunnel barrier and a Schottky barrier. In this respect surface states at the semiconductor surface are of importance because they can mediate charge flow through both barriers. In the limit of vanishing density of surface states, charge flows directly between metal and the semiconductor valence and conduction bands. Although this situation is encountered for the special case of a clean GaAs (110) surface, it is not likely to apply to the low-symmetry apex of a GaAs tip, particularly not if it has been exposed to air. We will therefore assume that a significant density of semiconductor surface states is present. Moreover, we use a uniform density of surface states throughout the band gap and describe their occupation using a surface electrochemical potential V_s. This can properly be assigned if the carriers are in thermal equilibrium. As indicated in Fig. 1, the potential zero is taken at the Fermi level in the semiconductor bulk, while the potential in the metal electrode is denoted by V_m. In the depletion region the energy bands are bending down (p-type GaAs) by an amount equal to V_{bb}, which is related to the Schottky barrier height Φ_s by

$$V_{bb} = \Phi_s - V_s - \xi, \tag{5}$$

where ξ is the difference between the Fermi level and valence-band maximum in the semiconductor bulk. Φ_s is defined as the difference between the *surface* quasi-Fermi level and the position of the valence-band edge at the semiconductor *surface*.[23]

As already stated, the semiconductor surface states play a central role in transport across the junction. They will not only determine the charge exchange between the metal and semiconductor surface via tunneling, but also communicate with the semiconductor bulk bands. Communication with the bulk valence band requires current over or through the Schottky barrier, together with recombination or energy relaxation at the semiconductor surface. This will be referred to as the Schottky current. Charge flow between surface states and conduction band only has to be taken into account when a substantial amount of minority carriers is present in the conduction band. This happens, for instance, in the case of photoexcitation, resulting in a so-called photocurrent. In the following we will give expressions for these semiconductor subsurface currents, for each spin component, in terms of

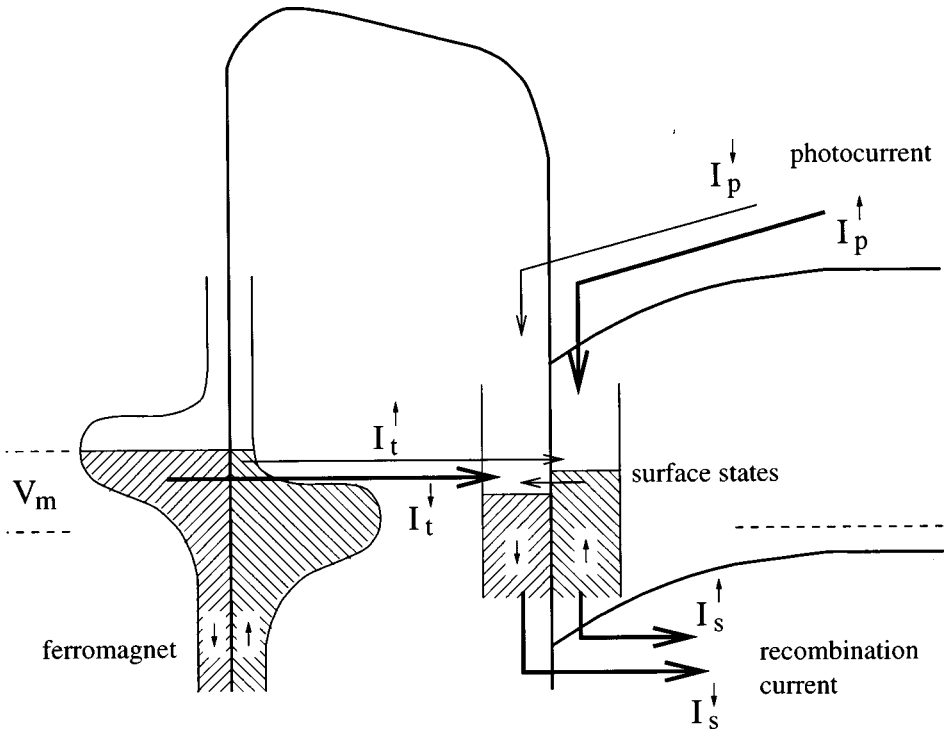

FIG. 2. Schematic overview of the spin-polarized *electron* flows in a ferromagnet/semiconductor tunnel junction under optical excitation. Arrows indicate, for both spin directions, the *electron* flow associated with the photocurrents $I_p^{\uparrow}$ and $I_p^{\downarrow}$, the Schottky currents $I_s^{\uparrow}$ and $I_s^{\downarrow}$, and the tunnel currents $I_t^{\uparrow}$ and $I_t^{\downarrow}$. For the forward bias case shown, electrons tunnel from filled (shaded) states in the ferromagnet (on the left) into empty surface states located in the semiconductor band gap. The tunnel current polarization is determined by the polarization of the ferromagnets states and the spin imbalance in the occupation of the semiconductor surface states.

the semiconductor surface potentials $V_s^{\uparrow}$ and $V_s^{\downarrow}$. In addition, spin relaxation in the semiconductor surface states is considered. A schematic representation of the spin-dependent currents is given in Fig. 2, showing the case of forward bias, in which electrons tunnel from filled states in the ferromagnet (on the left) into empty surface states located in the semiconductor band gap (on the right). Note the spin imbalance in the semiconductor surface states and the small arrow, pointing from the spin-down to the spin-up surface states, which denotes spin relaxation at the semiconductor surface, to be discussed below.

1. Schottky current

For the description of the Schottky current, we will limit ourselves to the case where the dominant transport mechanism is the thermally assisted emission of majority carriers (holes) from the bulk valence band to the surface, known as thermionic emission. This situation occurs in high mobility semiconductors, such as GaAs, at not too high doping density (a few times 10^{23} m^{-3} and lower). Ignoring spin for the moment, the Schottky current density J_s from semiconductor surface to bulk is given by[24–26]

$$J_s = J_0[\exp(\beta V_s) - 1], \quad J_0 \equiv -A^{**}T^2\exp(-\beta\Phi_s), \tag{6}$$

where J_0 is the saturation current density and A^{**} is the effective Richardson constant.[24–26] T is the temperature (in K) and $\beta = -e/k_BT$ with k_B the Boltzmann constant. Small deviations from the thermionic emission equation, due to the presence of other transport mechanisms (tunneling through the Schottky barrier at higher doping levels), can be incorporated by adopting a slightly different current expression

$$J_s = J_0\exp(\beta V_s/n)[1 - \exp(-\beta V_s)] \tag{7}$$

where n is the ideality factor. For $n=1$ we recover Eq. (6).

The most important feature is the exponential dependence of the Schottky current on the voltage difference V_s between semiconductor surface and bulk. This is caused by the influence of bias on the degree of band bending. For forward bias ($V_s<0$) the band bending is reduced and the current increases exponentially with voltage. For reverse bias ($V_s>0$) the bands are bent further down and the current experiences an increasing resistance. This rectifying behavior is reduced when n deviates from unity.

The application of voltages not only induces a thermionic emission current, but also implies charge rearrangements at the semiconductor surface. This shifts the surface Fermi level with respect to the semiconductor bands and modifies the Schottky barrier height Φ_s. To first order in V_m and V_s, the barrier height is given by

$$\Phi_s = \Phi_s^0 - \frac{\tilde{C}_t[V_m - V_s] - \tilde{C}_s V_s}{\tilde{C}_t + \tilde{C}_s + e^2 D_{ss}} \equiv \Phi_s^0 - \gamma_t[V_m - V_s] + \gamma_s V_s, \tag{8}$$

where Φ_s^0 is the barrier height in the equilibrium state (when $V_m = V_s = 0$), $\tilde{C}_t$ and $\tilde{C}_s$ are the capacitances per unit area of the tunnel and Schottky barrier, respectively, and D_{ss} is the density of surface states (units m^{-2} J^{-1}). The γ factors are defined as $\gamma_t \equiv \tilde{C}_t/[\tilde{C}_t + \tilde{C}_s + e^2 D_{ss}]$ and $\gamma_s \equiv \tilde{C}_s/[\tilde{C}_t$

$+\tilde{C}_s+e^2D_{ss}]$ and have values between 0 and 1. Equation (8) tells us how at the surface, the position of the valence-band edge shifts with respect to the surface quasi-Fermi level, in response to the drop of electrochemical potential across the tunnel barrier (weighted by the factor γ_t) and in response to the potential drop across the Schottky barrier (weighted by the factor γ_s).

Equations (5) and (8) can be combined into

$$V_{bb}=V_{bb}^0-\gamma_t V_m-[1-\gamma_t-\gamma_s]V_s \quad \text{with} \quad V_{bb}^0=\Phi_s^0-\xi. \tag{9}$$

The first term (V_{bb}^0) represents the band bending in the equilibrium state. The second term describes the dependence of the band bending on the external bias (V_m). In the case of a limited density of surface states, the semiconductor subsurface region is not completely shielded from the metal, such that the applied bias V_m influences the band bending in the semiconductor by a capacitive coupling.[27–29] The third term takes account of the band bending caused by the drop of electrochemical potential V_s across the Schottky barrier, which is nonzero only in the case of current in the semiconductor.

As regards the polarization of the Schottky current, it is important to realize that for thermionic emission the relevant quantity is the energy difference between the electrochemical potential and the maximum of the Schottky potential barrier. This positions the tail of the Fermi-Dirac distribution with respect to the barrier maximum and determines, together with temperature, the number of carriers that are able to be emitted over the barrier. Concerning spin dependence, we note that band bending and the formation of a space-charge layer is entirely governed by electrostatics. Here only the electron charge, not spin, is of importance. The band bending is thus controlled by the spin-averaged potential $\overline{V_s}$ and given by [compare to Eq. (9)]

$$V_{bb}=V_{bb}^0-\gamma_t V_m-[1-\gamma_t-\gamma_s]\overline{V_s}. \tag{10}$$

The spin polarization of thermionic emission is thus produced by the spin dependence of the electrochemical potentials.[30] The electrochemical potential at the semiconductor surface as well as that in the bulk has to be considered, for the net Schottky current is the difference between a component from semiconductor bulk to surface and one flowing in the opposite direction (see also Appendix A). The former is governed by the bulk carrier distribution, the latter by the surface level occupation. For the surface we have already argued that spin-dependent potentials $V_s^{\uparrow}$ and $V_s^{\downarrow}$ arise from optical orientation. In the bulk, in principle also the valence-band holes become polarized under optical orientation. However, the density of optically created holes is usually negligible compared to the dopant-induced hole density. Moreover, due to the spin-orbit interaction, a strong coupling exists between hole spin and its momentum $\vec{k}$, resulting in a loss of the hole spin orientation on the time scale of the momentum relaxation time ($\tau_p \sim 10^{-13}$s). We will therefore neglect the polarization of the bulk valence-band holes. Under these assumptions the thermionic emission currents J_s^{σ} for each spin are derived in appendix A, giving

$$J_s^{\sigma}=-\frac{1}{2}A^{**}T^2\exp[-\beta(V_{bb}+\xi+V_s^{\sigma})]\ \{\exp(\beta V_s^{\sigma})-1\}, \tag{11}$$

where V_{bb} is given by Eq. (10). Note that for the first term in curly brackets, corresponding to the emission of holes from the bulk, the spin variable drops out as it cancels with the prefactor.

2. Photocurrent

Upon irradiation with photons of energy higher than the band gap, electron-hole pairs are created in the semiconductor. Due to the internal electric field present in the near-surface depletion region, electrons and holes are spatially separated. The holes are driven into the semiconductor bulk, while the electrons are swept towards the surface. Hence a net current is established, hereafter referred to as the photocurrent. To calculate the photocurrent, we have to consider not only electrons generated in the depletion layer, but also those created deeper inside the semiconductor. These can reach the depletion region by diffusion and thereby contribute to the current too.

In the space-charge region we will neglect recombination losses since only a short time is needed to traverse this region. The contribution of electrons created in the space-charge layer can then be calculated by simply counting their number, considering the illumination intensity, light absorption, etc.[31] For the contribution of electrons created outside the depletion region, we have to solve the one-dimensional diffusion equation with suitable boundary conditions.[31] Adding the two terms yields for the total, spin-integrated photocurrent density J_p, from semiconductor surface to bulk,[31]

$$J_p=f_p\left\{1-\frac{\exp(-\alpha w)}{\alpha L_d+1}\right\}, \tag{12}$$

where α is the photon absorption coefficient and L_d is the minority carrier diffusion length, which is related to the diffusion coefficient D and the minority carrier lifetime τ via $L_d=\sqrt{D\tau}$. The prefactor f_p

$$f_p=\frac{e\,\eta_q P}{E_{ph}A_l}, \tag{13}$$

contains the quantum efficiency η_q for conversion of photons into electron-hole pairs ($0\leqslant\eta_q\leqslant 1$) and the incident flux of photons $P/E_{ph}A_l$, determined by the absorbed light power P, the photon energy E_{ph}, and the illuminated area A_l.

To include the spin variable, we have to discuss the concept of a photocurrent in more detail. In the present context, we describe the generation of a photocurrent as a two step process.[32] The first step is the optically induced transition of electrons from valence-band states to conduction-band states. The second step is the transport of the excited electrons to the surface. The spin polarization of the photocurrent depends on the initial polarization and spin relaxation during transport towards the surface. The spin polarization of conduction-band electrons just after excitation is determined by band-structure properties and selection rules for optical transitions induced by circularly polarized light. For a wavelength matched to the GaAs band gap, electrons are excited

from the Γ point ($k = 0$) only, resulting in a theoretical polarization of $\pm 50\%$. For smaller wavelengths, transitions from states away from the center of the Brillouin zone contribute and the spin polarization is slightly lower. At even shorter wavelength, transitions from the spin-orbit split-off band start mixing in, reducing the polarization severely. In our model we denote the fraction of excited spin-up and spin-down electrons by $C^{\uparrow}$ and $C^{\downarrow}$, respectively, with the condition $C^{\uparrow}+C^{\downarrow}=1$. For band-gap excitation in GaAs with right-handed circularly polarized light, we have $C^{\uparrow}=3/4$ and $C^{\downarrow}=1/4$, while for left-handed circularly polarized light we get $C^{\uparrow}=1/4$ and $C^{\downarrow}=3/4$.

During transport to the surface, the polarization is reduced as a result of spin relaxation. Two mechanism are most relevant, depending on temperature and doping density.[33] The first one is the D'yakonov-Perel' mechanism, which is efficient in bulk GaAs at higher electron kinetic energy. The second mechanism, proposed by Bir, Aronov, and Pikus, is related to electron-spin scattering by holes and therefore scales with the GaAs doping density. Values for the spin-relaxation time in GaAs, determined from measurements of the circular polarization of luminescence, are about 5×10^{-11} s at 300 K (with little dependence on doping concentration) and range below 77 K from 2×10^{-10} s at high doping density to 2×10^{-9} s at low doping density.[33]

The effect of spin relaxation during drift in the band-bending region is negligible since electrons travel at velocities above 10^5 m/s through this region generally smaller than 100 nm. This takes less than 1 ps, a time much shorter than the lower limit of the spin-relaxation time (50 ps). Electrons created in the depletion region will therefore reach the semiconductor surface with virtually the same spin polarization as just after excitation. The photocurrent J^{σ}_{depl} from electrons excited in the depletion region is then easily evaluated from expressions given previously for the spin-integrated current,[31] giving

$$J^{\sigma}_{depl}=C^{\sigma}f_p\{1-\exp(-\alpha w)\}. \tag{14}$$

For electrons created deeper inside the semiconductor, spin relaxation is important during diffusion towards the depletion region. A spin-dependent diffusion photocurrent J^{σ}_{dif} is therefore included in the model. In Appendix B it is shown that the polarization of the diffusive photocurrent can be expressed in terms of the minority carrier diffusion length $L_d=\sqrt{D\tau}$ and a ''spin-asymmetry'' diffusion length L_s. The latter is given by $L_s=\sqrt{D\tau/(1+\tau/\tau_s)}$, where τ_s is the spin-relaxation time. The polarization P_{dif} of the diffusive photocurrent is given by (Appendix B)

$$P_{dif}=\left(\frac{C^{\uparrow}-C^{\downarrow}}{C^{\uparrow}+C^{\downarrow}}\right)\left(\frac{\alpha+1/L_d}{\alpha+1/L_s}\right). \tag{15}$$

For a long spin-relaxation time ($\tau_s \gg \tau$) we have $L_s=L_d$ and the polarization is given by the value at excitation. When the spin-relaxation time becomes comparable to or shorter than the minority carrier lifetime, the polarization of the diffusion photocurrent is diminished. The reduction can be significant; using typical values for GaAs, $\alpha=1\ \mu\text{m}^{-1}$, $L_d=2\ \mu$m, and $\tau=7\times10^{-9}$ s, the polarization is reduced by roughly a factor of 3 for $\tau_s=1\times10^{-10}$ s. The diffusion photocurrents J^{σ}_{dif} are explicitly written as (Appendix B)

$$J^{\sigma}_{dif}=\frac{1}{2}f_p\exp(-\alpha w)\left\{\frac{\alpha L_d}{\alpha L_d+1}\pm\frac{\alpha L_s}{\alpha L_s+1}(C^{\uparrow}-C^{\downarrow})\right\}, \tag{16}$$

where the plus sign should be used for $\sigma=\uparrow$ and the minus sign for $\sigma=\downarrow$. From Eqs. (14) and (16) one can obtain the total photocurrent $J^{\sigma}_{depl}+J^{\sigma}_{dif}$ for each spin orientation. Simple algebra shows that the sum of both spin channels can be rewritten in the form previously given for the total photocurrent J_p in Eq. (12).

Summarizing, in GaAs the polarization of electrons created in the depletion region is hardly reduced during transport to the surface. Spin relaxation is important however for the diffusive contribution. This picture is supported by measurements of the spin polarization of photocurrents extracted from thin GaAs layers.[34] For films of 0.2 μm thickness a maximum polarization of 49% was found, close to the theoretical value. Thicker layers produced a lower maximum polarization, attributed to the increasing effect of spin relaxation for electrons created further away from the surface.

3. Spin relaxation in surface states

When electrons reside in surface states, they can flip their spin at a certain rate. If a spin imbalance in the occupation of the surface states exists, then on the average a larger number of spin flips per unit time will occur for the spin that is dominantly present. This results in a net flow of electrons from one to the other spin subsystem. We define the excess density of spin up electrons[35] as $N_{exc}=-e(V_s^{\uparrow}-V_s^{\downarrow})D_{ss}/2$. Denoting the surface state spin lifetime by τ_{ss}, the density of current J_{flip} from the spin-up to the spin-down subsystem is written as

$$J_{flip}=\frac{-eN_{exc}}{\tau_{ss}}=\frac{e^2D_{ss}}{2\tau_{ss}}(V_s^{\uparrow}-V_s^{\downarrow}). \tag{17}$$

In effect, this spin-flip current tends to minimize the spin splitting in the surface electrochemical potential.

Having discussed the spin polarization of the current components, we can now write down the conditions for charge and spin conservation:

$$\begin{aligned} J_p^{\uparrow}+J_s^{\uparrow}-J_t^{\uparrow}+J_{flip}&=0,\\ J_p^{\downarrow}+J_s^{\downarrow}-J_t^{\downarrow}-J_{flip}&=0. \end{aligned} \tag{18}$$

Due to the fact that J_{flip} contains both the unknown variables $V_s^{\uparrow}$ and $V_s^{\downarrow}$ to be calculated, the two equations are coupled and have to be solved simultaneously in a self-consistent manner.

In one particular limiting case we can derive an analytical expression for the splitting $(V_s^{\uparrow}-V_s^{\downarrow})$ in the surface state potential. Two basic assumptions have to be made: (i) The tunnel current can be neglected compared to the photocurrent and Schottky current, and (ii) the surface spin splitting is small enough so that we can neglect the polarization of the Schottky current ($J_s^{\uparrow}\approx J_s^{\downarrow}$). Eqs. (18) can then be combined to $J_p^{\uparrow}-J_p^{\downarrow}=-2J_{flip}$. Using expression (17) for J_{flip} we get

$$V_s^{\uparrow} - V_s^{\downarrow} = -\frac{\tau_{ss}}{e^2 D_{ss}}(J_p^{\uparrow} - J_p^{\downarrow}). \tag{19}$$

Next we use Eq. (4) to evaluate the modulation ΔI_t of the tunnel current due to a modulation of the circular light polarization. In the limit under consideration we have, because of symmetry, $\Delta V_s^{\uparrow} = -\Delta V_s^{\downarrow}$ and $\Delta V_s^{\uparrow} \equiv (V_s^{\uparrow} - V_s^{\downarrow})/2$. Inserting this in Eq. (4) yields, together with Eq. (19),

$$\Delta I_t = \frac{\tau_{ss}}{2e^2 D_{ss}}(J_p^{\uparrow} - J_p^{\downarrow})(G_t^{\uparrow} - G_t^{\downarrow}). \tag{20}$$

The modulation signal thus scales with the polarization of photocurrent and tunnel conductance and is inversely proportional to the surface state spin-flip rate.[36] In the next section we will see that this situation is approached for high enough forward bias, where the junction is operated in the photovoltaic regime.[13,8]

III. CALCULATION RESULTS

A. Calculation procedure and parameters

Based on the model for spin-polarized transport, we can calculate the difference in tunnel current for excitation with left- or right-handed circularly polarized light. This quantity will hereinafter be referred to as the circular polarization modulation (CPM) signal. In addition, we can evaluate the change in current in response to a small variation of the light intensity. We will call this the intensity modulation (IM) signal. The latter is important because experimentally it is not trivial to modulate the circular polarization without introducing at the same frequency also an intensity modulation. Possible sources are imperfect alignment of the optical components, polarization-dependent optical scattering in the tunnel junction, or magneto-optical effects due to interaction of the light with the magnetic sample. An intensity modulation can translate into a current modulation in three ways. First, there is the change of the photocurrent magnitude, which directly influences the tunnel current. Second, heating effects can cause a modulation of the tip to sample separation. Third, a modulation in the semiconductor surface potential may occur, causing displacement currents through the junctions capacitance. A detailed account of all three components was given in Ref. 13, where time-dependent currents were described with help of complex admittances $Y = G + j\omega C$, with ω the modulation frequency.

To determine the CPM and IM signals, we adopt a quasistatic approach, in which we calculate for two laser intensities, differing by 5%, the direct currents for both left and right circularly polarization. The modulation signals are then obtained by taking appropriate combinations of the currents in the four situations. The procedure thus ignores displacement currents[37] and does not include phase changes produced due to capacitances in the junction. In the IM signal we have also not included modulations due to heating.

The modulation signals, together with the time-averaged total tunnel current, have been calculated as a function of the externally applied bias V_m. We used several values of the tunnel conductance polarization and spin-relaxation time τ_{ss}. Also the influence of bulk spin scattering of photoelectrons is studied by varying the parameter τ_s. Values used for the other parameters are collected in Table I. For material parameters, marked by 1 in the last column, we have taken literature values for GaAs. Parameters marked 2 are dictated by the experimental conditions.[38] The two γ factors are calculated from a combination of several constants.

TABLE I. Values for the parameters used in the model calculation. 1 denotes material parameters and 2 denotes parameters dictated by experimental conditions.

Parameter	Value	Source
V_{bb}^0	-0.39 V	1,2
ξ	-0.1 V	1
N	5×10^{23} m^{-3}	2
A^{**}	10^6 A m^{-2} K^{-2}	1
T	300 K	2
D_{ss}	1×10^{36} m^{-2} J^{-1}	1,2
τ	7.2×10^{-9} s	1
L_d	2×10^{-6} m	1
P	0.5×10^{-3} W	2
A_l	3.14×10^{-10} m^2	2
E_{ph}	1.55 eV	2
α	1×10^6 m^{-1}	1
η	1	1
β	38.7 V^{-1}	2
γ_t	0.23	
γ_s	0.09	

B. Results

Let us first illustrate the relationship between CPM signal and the polarization of the tunnel conductance (read sample magnetization). To do so, we have calculated the CPM and IM signals for different values of $G_t^{\uparrow} - G_t^{\downarrow}$, while keeping the total tunnel conductance $G_t^{\uparrow} + G_t^{\downarrow}$ constant. The maximum polarization used was 30%, which is close to the value detected for Co in spin-polarized transport measurements with thin-film tunnel junctions.[39] For the photocurrent we used 50% polarization at excitation and a bulk spin lifetime τ_s equal to 1×10^{-10} s. This gives a net photocurrent polarization of 16%. The results are shown in Fig. 3, with the CPM signal plotted in arbitrary units as we do not yet want to emphasize the signal magnitude at this point. The precise value of the surface spin-relaxation time τ_{ss} is therefore not relevant here.

As expected, we see that the CPM signal (upper plot) is proportional to the tunnel conductance polarization and reverses sign when the conductance polarization is inverted (see also Ref. 21). Moreover, the signal magnitude exhibits a distinct dependence on bias voltage. In fact, the signal completely disappears for higher positive (reverse) bias, irrespective of the tunnel conductance polarization. In contrast, the IM signal (middle plot) shows exactly the opposite behavior, approaching zero for the bias polarity where the CPM signal is largest. The remarkable variation with V_m is correlated with the deviation of the total tunnel current (bottom plot) from a linear curve. The negative (forward) bias part of the

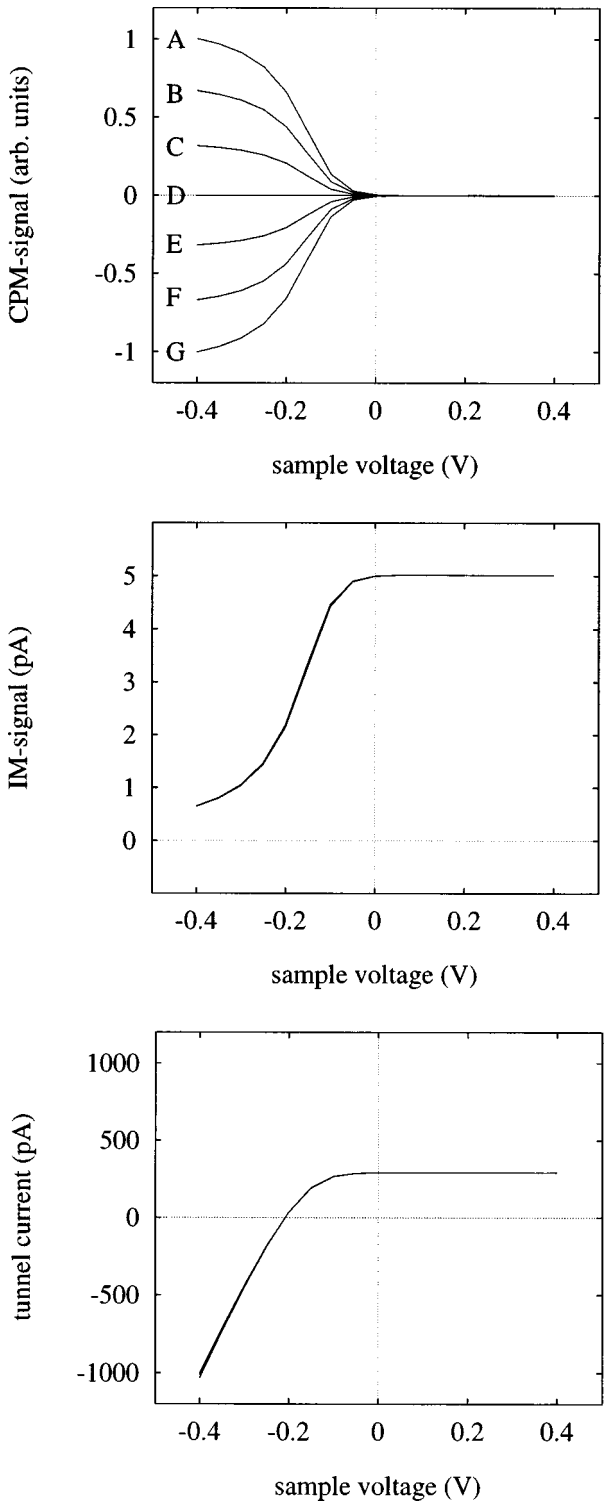

FIG. 3. Calculated CPM signal (upper plot) as a function of bias V_m, for tunnel conductance polarizations $(G_t^{\uparrow}-G_t^{\downarrow})/(G_t^{\uparrow}+G_t^{\downarrow})$ of 30%, 20%, 10%, 0%, −10%, −20% and −30% for curves $A-G$, respectively. The total tunnel conductance $(G_t^{\uparrow}+G_t^{\downarrow})$ and all other variables are kept constant. The middle and lower plots show the IM signal and the total tunnel current, respectively, obtained with the same parameter settings.

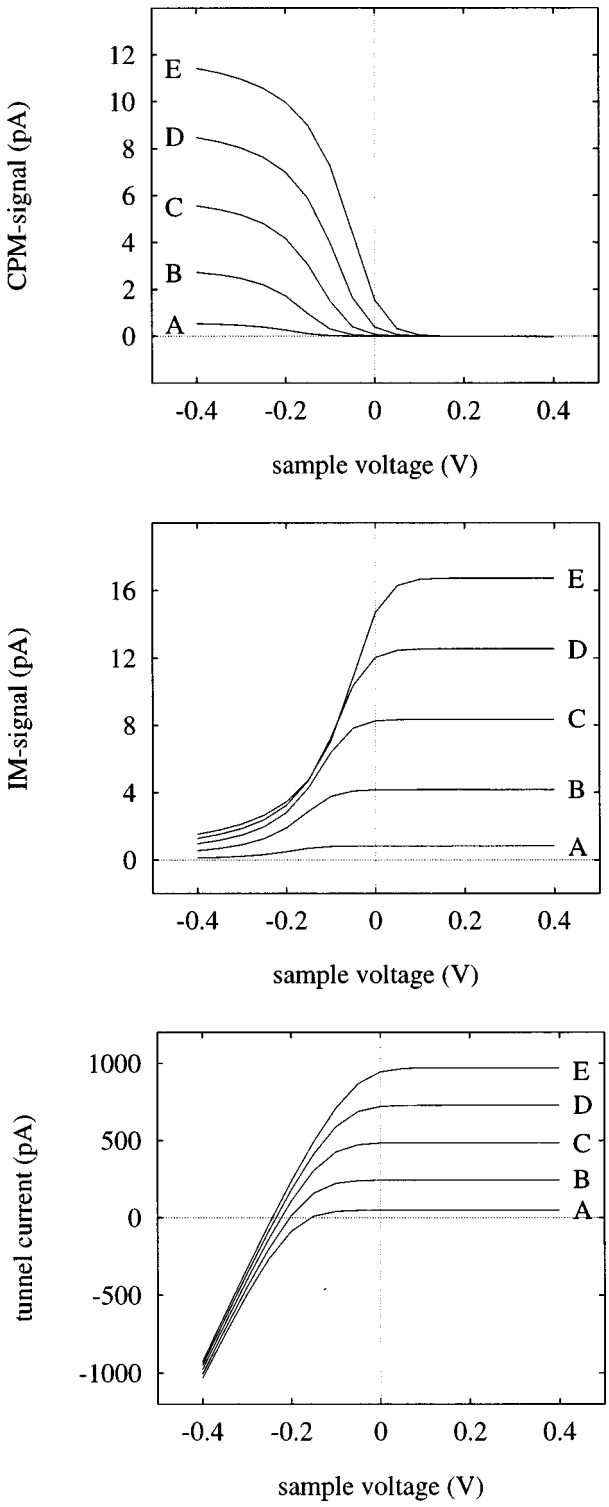

FIG. 4. Calculated CPM signal (upper plot) with the total photocurrent varied, for a 30% polarization of the tunnel conductance. The middle and lower plots show the IM signal and the total tunnel current, respectively, obtained with the same parameter settings.

curve is linear, while the slope of the curve is reduced to zero at reverse bias. The current saturation at reverse bias is caused by the finite supply of photoelectrons, which limits the tunnel current (see also Ref. 13). We will explain the relation with the modulation signals after having discussed the effect of the total tunnel conductance and photocurrent on the modulation signals.

Figure 4 shows results obtained for a varying size of the total photocurrent $(J_p^{\uparrow}+J_p^{\downarrow})$, keeping its polarization fixed. Experimentally this is achieved by changing the incident

light power. The power was chosen such that saturation of the current occurs at reverse bias ($V_m>0$), giving a deviation from a linear current voltage curve (lower plot). The increase of the saturation current at reverse bias for higher light power clearly shows that the amount of optically created carriers is the limiting factor in this regime. For larger light power, the linearly sloped part of the current extends up to higher positive bias. At the same time, the bias where the IM signal starts to increase and the CPM signal starts to decay shifts to the right. This convincingly shows that the variation of the modulation signals with bias is linked to the saturation of the current. The curves in Fig. 4 also show that increasing the laser power enhances the CPM signal at forward bias, though the total tunnel current is hardly affected. Hence the relative CPM effect is enlarged.

The link between tunnel current saturation and decay of the CPM signal also appears when the value of the total tunnel conductance ($G_t^{\uparrow}+G_t^{\downarrow}$) is varied. This can experimentally be done by changing the tip to sample distance. Figure 5 presents calculated curves, obtained with identical light intensity. First of all, at forward bias ($V_m<0$), the total tunnel current as well as the modulation signals decrease when the tunnel conductance is reduced. This is not surprising but not trivial since the statement does not, for instance, hold for positive bias voltages. In addition to this, we see in the lower plot for the total current a transition from a situation with current saturation as before (curve A) to a situation with a completely linear I-V characteristic (curve E). The latter happens for the lowest tunnel conductance, where the tunnel barrier limits the current over the complete voltage range shown here. The transition can also be seen in the modulation signals and for the smallest tunnel conductance, these become independent of the bias voltage. Thus, for low tunnel conductance, the characteristic variation of the CPM and IM signal due to the influence of the subsurface currents in the semiconductor is absent. In that case the CPM signal is proportional to a constant times the tunnel conductance polarization, where the constant is independent of bias voltage. Since in our calculations we have also used a constant value for the tunnel conductance polarization, we get the same CPM signal for all bias voltages. The interesting feature about this regime is that it allows one to associate a measured variation of the CPM signal with V_m, with the bias dependence of the tunnel conductance polarization, without the obscuring effect related to the semiconductor subsurface currents.

The decay of the CPM signal when the tunnel current saturates can be understood in the following way. At reverse bias ($V_m>0$), the bending of the semiconductor bands is enhanced. Therefore, thermionic emission of holes over the Schottky barrier becomes increasingly more difficult. Photoexcited electrons arriving at the surface then find only a small number of emitted valence band holes to recombine with, i.e., $I_s\approx 0$. Photoexcited electrons will therefore accumulate in the surface states and build up a considerable voltage V_s (with a negative sign). As a result, the voltage drop V_m-V_s over the tunnel barrier increases and thus the tunnel current. This continues until the tunnel current exactly balances the current of photoexcited electrons towards the surface. At this point a steady state is reached in which $I_t=I_p$ and the tunnel current is limited by I_p. To discuss the implications of this situation for the measured CPM signal, we note that the CPM signal results from a modulation of the polarization of the photocurrent, without changing its total size. Since we are in the regime where the Schottky current

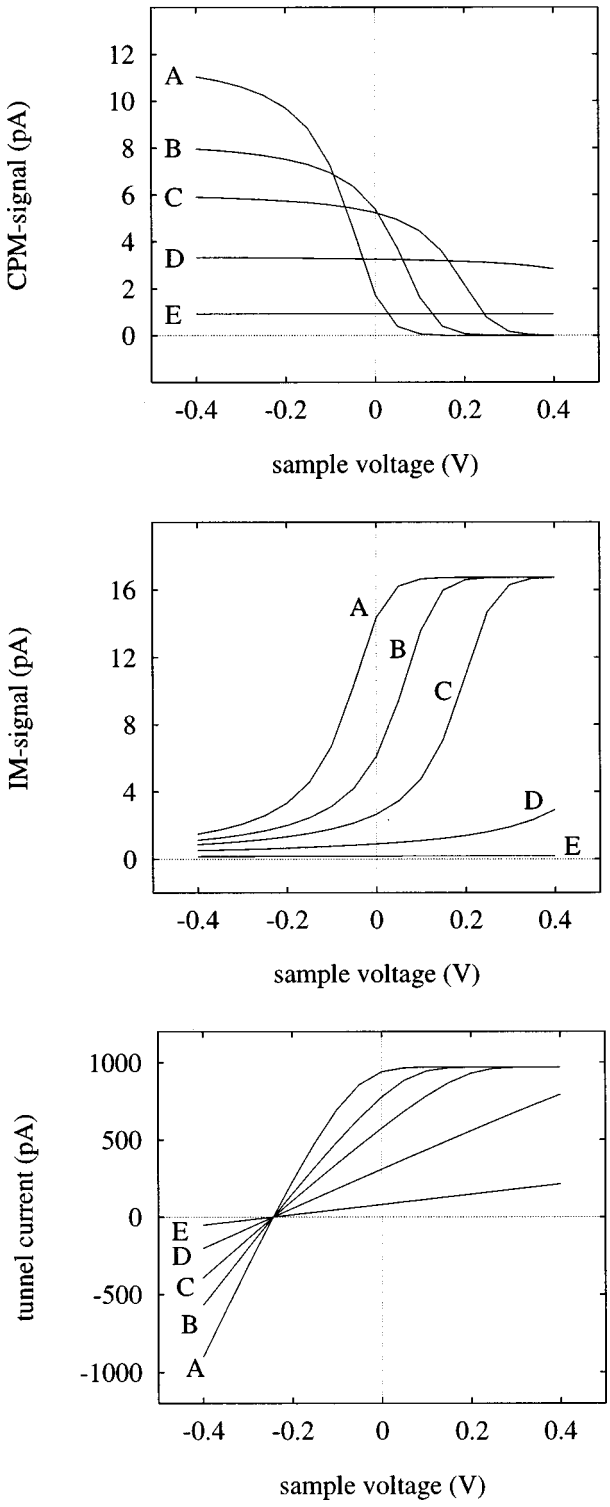

FIG. 5. Calculated CPM signal (upper plot) with the total tunnel conductance as the parameter, for a 30% polarization of the tunnel conductance. The middle and lower plots show the IM signal and the total tunnel current, respectively, obtained with the same parameter settings.

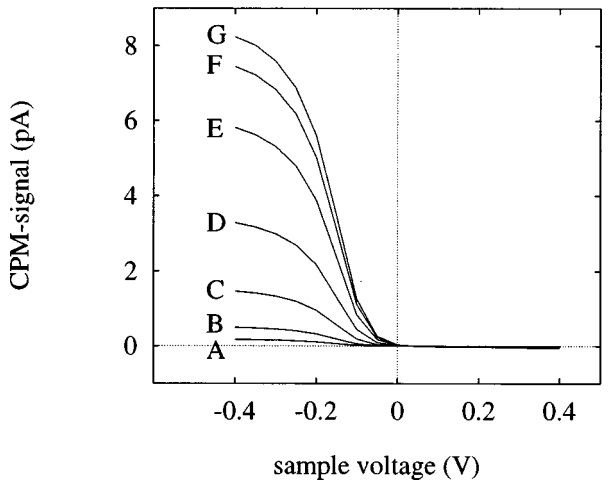

FIG. 6. Calculated CPM signal for various surface spin lifetimes τ_{ss}. The values are 1×10^{-10} s (A), 3×10^{-10} s (B), 1×10^{-9} s (C), 3×10^{-9} s (D), 1×10^{-8} s (E), 3×10^{-8} s (F), and 1×10^{-7} s (G). The IM signal and the total tunnel current (not shown) behave essentially the same as before and are virtually identical for all values used for τ_{ss}.

is negligible and $I_t=I_p$, the modulation cannot result in a change of the *total* current. Hence the CPM signal has to be zero.

We stress, however, that this does not necessarily mean that the tunnel current is *not polarized*. To illustrate this we discuss each spin channel separately. This is most easily done in the absence of spin-flip processes at the semiconductor surface. In that case both spin channels are independent of each other and for each spin orientation, the surface potential V_s^σ will adjust itself to satisfy the condition $I_t^\sigma=I_p^\sigma$. This condition has to be satisfied irrespective of the supply of photoexcited electrons and the size of the tunnel conductance for each spin, which naturally leads to a polarization of the tunnel current equal to that of the photocurrent. We thus have the remarkable situation that we have no CPM signal, while the tunnel current polarization is nonzero and changes sign when the excitation light is changed to the other circular polarization. The story stays essentially the same in the case spin flips occur. For example, if a large amount of spin-up photoelectrons arrives at the surface and the tunnel conductance for this spin happens to be small, then most of them can still tunnel via the spin-down conductance channel after having flipped the spin. The polarization of I_t, however, is then smaller than that of I_p.

The influence of the surface state spin-relaxation time τ_{ss} was examined using values ranging from 1×10^{-10} s to 1×10^{-7} s. The resulting CPM signal is displayed in Fig. 6 for a tunnel conductance polarization of 30%. The calculation reveals a drastic effect of τ_{ss} on the magnitude of the CPM signal. For the shortest spin lifetimes used, the CPM signal is smaller than 0.2 pA, where the total tunnel current is 1 nA (not shown). The relative effect is thus only 0.02%. For larger τ_{ss}, the modulation signal rapidly increases, which demonstrates the importance of having a small spin-flip rate in the semiconductor surface states. For longer spin lifetimes (above a few times 10^{-8} s), the CPM signal becomes only weakly dependent on τ_{ss} and eventually saturates. In this situation the signal is determined only by the polarization of tunnel conductance and photocurrent.

TABLE II. Exact numerical value (second column) of the CPM signal at $V_m=-0.4$ V for several values of τ_{ss}, compared to the value computed from the approximate analytical expression (20) in the third column. The parameters are the same as for Fig. 6.

τ_{ss} (s)	CPM signal (pA)	ΔI_t (pA)
1×10^{-7}	8.2	197
3×10^{-8}	7.4	59
1×10^{-8}	5.8	20
3×10^{-9}	3.3	5.9
1×10^{-9}	1.46	2.0
3×10^{-10}	0.50	0.59
1×10^{-10}	0.17	0.20

It is interesting to compare the exact numerical results with that given by the approximate analytical expression (20) derived in Sec. II. Values determined from the latter are given in Table II, together with the exact numerical result at $V_m=-0.4$ V, as shown already in Fig. 6. It is noted that for short spin-relaxation times τ_{ss}, the numerical result approaches the approximate value at $V_m=-0.4$ V. For larger time constants the analytical expression grossly overestimates the CPM signal. The approximation fails for large τ_{ss} because then the surface spin splitting in V_s becomes so large that the polarization of the Schottky current can no longer be neglected. A Schottky current with significant polarization tends to reduce the spin splitting in V_s, just as spin-flip processes in the surface states do.

Furthermore, note that even for short τ_{ss}, the approximate value overestimates the exact numerical result at small forward (negative) bias or at reverse (positive) bias. In Fig. 6 we can see that at these bias voltages the CPM signal is much smaller than the value at $V_m=-0.4$ V given in Table II. Thus a further requirement for the approximation to hold is that the junction is operated in the photovoltaic regime at large enough forward bias. Only then does the tunnel current hardly disturb the currents in the semiconductor subsurface region and can tunneling be neglected in calculating the semiconductor surface potentials. The surface potentials V_s^σ are then primarily determined by the photocurrent and Schottky current, where the latter becomes large because the band bending is strongly reduced due to the applied voltage. Summarizing, the assumptions underlying Eq. (20) are valid in the photovoltaic regime for short spin lifetime τ_{ss}.

The last important variable in our model is the spin lifetime τ_s of minority carriers in the bulk of the semiconductor. This determines the depolarization of photoelectrons during diffusive transport to the surface[40] and thereby the net polarization of the photocurrent. We have varied τ_s from 10^{-6} s to 10^{-11} s and calculated the corresponding photocurrent polarization and CPM signal. The total photocurrent is kept constant. The results are presented in Table III.

For the range of values used for τ_s, the photocurrent polarization varies from 50% for the largest spin lifetime to 7.4% for $\tau_s=10^{-11}$ s. As expected we see that for spin lifetimes longer than the minority carrier lifetime $\tau=7\times10^{-9}$ s, the photocurrent polarization and thus the CPM signal is hardly affected by bulk spin scattering. For smaller spin life-

TABLE III. Photocurrent polarization and CPM signal for several values of τ_s, at bias voltage $V_m = -0.4$ V.

τ_s (s)	Polarization (%)	CPM signal (a.u.)
1×10^{-6}	50	1
1×10^{-7}	49	0.99
1×10^{-8}	46	0.91
1×10^{-9}	32	0.64
1×10^{-10}	16	0.32
1×10^{-11}	7.4	0.15

time the CPM signal is reduced in proportionality to the photocurrent polarization. The overall dependence of the CPM signal on τ_s is relatively weak, with a reduction of the CPM signal of less than a factor of 2 when τ_s is reduced by an order of magnitude. Since spin depolarization is considered only for the diffusive contribution to the photocurrent, the effect might be even weaker in the case where this component is only a minor fraction of the total photocurrent. As can be seen from Eqs. (14) and (16), this fraction is controlled by the depletion width w and the light absorption coefficient α.

IV. DISCUSSION

In the preceding section we have presented the calculated dependence of the modulation signals on the various parameters and variables involved. The most important parameter is the tunnel conductance polarization since this quantity reflects the magnetic properties of the sample under investigation. The CPM signal was shown to be proportional to the tunnel conductance polarization and changes sign when the conductance polarization does. Hence the CPM signal is a measure of the samples magnetic structure and spatial variations in the surface magnetization of the sample should appear in the CPM signal. Since the signal is produced by a modulation of the tunnel current, the spatial resolution in the CPM signal in STM is in principle the same as for the total tunnel current. Magnetic resolution at the atomic scale should therefore be feasible.

In a similar way the CPM signal was shown to scale with the polarization of the photocurrent. The latter is governed by the bulk spin lifetime τ_s and it is therefore advantageous to have low spin depolarization in the semiconductor bulk. Yet the net effect on the CPM signal is relatively weak, especially in the regime where τ_s becomes comparable to or larger than the minority carrier lifetime τ. In that case electrons can escape from the photocurrent through recombination with valence-band holes before they have had a chance to relax their spin.

A much stronger influence on the CPM signal has the spin lifetime τ_{ss} of electrons in the semiconductor surface states. Except for very long surface spin lifetimes (above 10^{-8} s), the CPM signal goes down linearly with decreasing spin lifetime. The general picture is that when the surface state spin lifetime is short, photoelectrons will have lost their spin orientation before they can leave the surface states. The tunnel current is then drawn from a reservoir of hardly polarized electrons and no spin sensitivity is expected. In essence, the situation is similar to that discussed above for the bulk spin relaxation, where the ratio of carrier lifetime and bulk spin lifetime determines the depolarization. In the surface states, the role of bulk minority carrier recombination is replaced by two different processes by which electrons can escape from the surface states before spin relaxation. The two channels are tunneling into the magnetic sample or recombination with thermionically emitted valence-band holes. The effect of spin relaxation is suppressed when the tunnel current or Schottky current is large.

The last point brings us to a more general feature of current modulation in tunnel junctions between a ferromagnet and a photoexcited semiconductor. This is the crucial role played by the balance of the relevant current components, namely, photocurrent, tunnel current, Schottky current, and current associated with spin flips in semiconductor surface states. The importance of this balance for the size of the CPM signal is most salient in the bias dependence of the modulation signals. This arises from bias-induced modification of the band bending and thereby of the Schottky current. Two regimes can be distinguished. In the photoamperic mode of operation, the Schottky current is, due to large band bending, negligible compared to the tunnel current. The tunnel current is then limited by the supply of photoexcited electrons and we have $I_t = I_p$. For this case we argued that no CPM signal can exist, even though the tunnel current can be highly polarized. Experimentally, this situation is established at reverse bias for suitably high tunnel conductance.

In the other regime, the photovoltaic mode of operation, the tunnel current is small compared to the Schottky current. Then the surface voltage V_s developing at the semiconductor surface is determined by the subsurface currents in the semiconductor, i.e., by the photocurrent and the Schottky current. The polarization of the tunnel current has in this case only a weak influence on the spin splitting $V_s^{\uparrow} - V_s^{\downarrow}$, as illustrated by the absence of G_t^{σ} in Eq. (19) derived for this regime. Instead, the surface spin splitting is exclusively determined by semiconductor variables, such as photocurrent polarization and surface state spin-flip rate. A nonzero CPM signal is then possible. The photovoltaic regime can experimentally be selected by using low tunnel conductance and high forward bias such that the semiconductor band bending is small.

Interestingly, the IM signal shows exactly the opposite behavior with bias voltage in comparison to the CPM signal. In the photovoltaic regime, the IM signal has only a small value while the CPM signal is largest. If, however, the junction is operated in the photoamperic mode, the CPM signal vanishes, but the IM signal becomes large. Thus, by choosing the right bias voltage, we can either set the junction to high spin sensitivity and low optical response (forward bias), or have only a small signal due to spin-polarized tunneling but a high response to small light intensity changes (reverse bias). Since our experiments aim at detection of a spin-polarized contribution to the tunnel current, without being sensitive to unwanted light intensity modulations, the preference for forward bias operation is evident. In contrast, for the measurement of magneto-optical effects in such junctions, a high optical response is required and it is best to use reverse bias. This has already been shown experimentally to facilitate imaging of prewritten magnetic bits in a Pt/Co multilayer sample with STM.[41]

With regard to material parameters that control the size of

the CPM signal, we have the polarization of the photocurrent and the spin lifetime in the semiconductor surface states (τ_{ss}). For a given GaAs tip these are fixed. In addition, we have the tunnel conductance polarization, which is actually the quantity one wants to extract from an experiment. To facilitate quantitative analysis of experimental data, it is desirable to have a simple relationship between the CPM signal on the one hand and tunnel conductance polarization, photocurrent polarization, and τ_{ss} on the other hand. Such a relationship exists [e.g., Eq. (20)] for the photovoltaic mode of operation, but it is only valid if τ_{ss} is small enough to neglect the polarization of the Schottky current. Conflicting requirements then arise since τ_{ss} should be as large as possible to have a maximum CPM signal. For large τ_{ss} Eq. (20) is no longer valid and the experimental data have to be compared with a numerical calculation involving more parameters (V_{bb}^0, γ_s, γ_t,...), thereby introducing additional uncertainties. It is therefore best to have experimental conditions such that Eq. (20) can be used, i.e., photovoltaic operation and negligible Schottky current polarization.Then the only uncertain factor is τ_{ss} since the photocurrent polarization can be derived from a measurement of the bulk spin lifetime, for which polarized luminescence techniques are available.[42]

Since the spin-flip rate at the semiconductor surface has such a drastic effect on the size of the CPM signal, experimental control over spin-flip processes is vital for the successful application of this method for spin-polarized tunneling in a STM. Some remarks about spin-relaxation mechanisms are therefore appropriate. Unfortunately, little is known about spin relaxation in surface states on semiconductors such as GaAs. Mechanisms active in bulk GaAs may be significantly modified or not present at all at the surface. Some idea might be obtained, however, from photoemission experiments on semiconductors with overlayers,[43–45] which indicate that the decay of polarization of photoemitted electrons due to spin scattering is particularly effective when the overlayer contains magnetic moments. For the native oxide on GaAs these are not expected to be present. For Cs/O overlayers on GaAs, depolarization was shown to be negligible,[42,46] suggesting that the spin lifetime is significantly larger than the time the emitted electron spends in the Cs/O layer. The latter is estimated to be about 10^{-13}–10^{-14} s, putting a lower limit of approximately 10^{-11} s on τ_{ss}.

Finally, we briefly discuss possible extensions of our model. The first one concerns the density of surface states D_{ss}, which we assumed to be uniformly distributed throughout the semiconductor band gap. Although sharp spectral features are probably not present in the case of a native GaAs oxide, some variation of D_{ss} with energy is likely. The most prominent consequence is that the spin-flip current [Eq. (17)] is no longer dependent only on the spin splitting in the semiconductor surface potential, but also on the average potential. This modifies the precise dependence of tunnel current polarization on bias, although the effect is of second order.

A second extention involves the consideration of a more realistic geometry for the STM junction, ideally fully three dimensional. Although the behavior in essence remains the same[13] as for the model of a planar junction, the ratio of the resistance of tunnel barrier and Schottky barrier is altered. Therefore, the regimes of photoamperic and photovoltaic behavior will occur for somewhat different parameters.

V. SUMMARY AND CONCLUSIONS

We have presented a theoretical model for spin-polarized transport in a tunnel junction consisting of a ferromagnet and a semiconductor in which spin-polarized carriers are created by optical orientation. The model includes, in addition to the tunneling current, the semiconductor subsurface currents, i.e., the current of photoexcited minority carriers and the Schottky current due to thermionic emission of holes. These have been split into components for the two different spin orientations and spin relaxation was included both in the semiconductor bulk and in the surface states. Charge flows were assumed to be mediated by a significant density of surface states for which a spin-dependent surface potential V_s^σ was defined.

The tunnel current was described in terms of a spin-dependent tunnel conductance G_t^σ and a voltage drop $V_m - V_s^\sigma$ over the tunnel barrier. The tunnel conductance G_t^σ takes account of the magnetic structure of the ferromagnetic electrode. The photocurrent consists of two contributions. The first originates from electrons created in the semiconductor depletion region and its polarization is determined by the polarization at excitation. The second contribution comes from electrons diffusing to the surface from deeper down in the semiconductor bulk. For this component spin depolarization due to a finite spin lifetime has been included. The equations for thermionic emission have also been rewritten to explicitly include the effect of a spin splitting in the surface potential V_s. For each spin, the current balance equations were given and solved self-consistently for $V_s^\uparrow$ and $V_s^\downarrow$. The total tunnel current and current modulations due to modulated optical orientation (CPM signal) or modulated light intensity (IM signal) were calculated as functions of the most important variables.

As expected, the CPM signal is proportional to the polarization of the tunnel conductance G_t and changes sign when G_t does. The magnitude of the CPM signal is lowered due to spin depolarization of photoelectrons in the semiconductor bulk. However, this effect is relatively weak. A more severe reduction of the CPM signal was shown to result from spin relaxation in semiconductor surface states.

The modulation signals display a distinct dependence on the bias voltage applied across the tunnel junction. Two regimes were distinguished. In the photoamperic mode, the tunnel current is limited by the photocurrent and the CPM signal vanishes, while the IM signal is large. This situation occurs at reverse bias for high enough tunnel conductance. In the second regime, where the junction is operated in the photovoltaic mode, the tunnel current has only a minor influence on the surface potentials V_s^σ. Instead, these are primarily determined by the semiconductor subsurface currents. In this regime the IM signal is small but the CPM signal is maximum. An approximate expression for the latter signal was shown to approach the exact numerical result in this regime. This situation can be established for forward bias and low tunnel conductance. The response to light intensity variations, given by the IM signal, thus has exactly the opposite behavior with changing bias. Regarding experiments, this leads to the important conclusion that forward bias is favorable for the detection of spin-polarized tunneling signals, with the smallest sensitivity for error signals produced by

unwanted light intensity modulations. This situation also allows quantitative extraction of the tunnel conductance polarization, provided the surface spin lifetime is known. The marked dependence of the CPM signal on bias voltage provides an additional experimental test of the origin of the measured signals. In conclusion, the model calculations provide significant insight into the spin-dependent transport in tunnel junctions under optical orientation and will be valuable for the interpretation of experimental results and for guiding future experiments.

ACKNOWLEDGMENTS

Part of this work was supported by the Stichting Fundamenteel Onderzoek der Materie (FOM), which is financially supported by the Nederlandse Organisatie voor Wetenschappelijk Onderzoek (NWO). The research was also supported by the European Community, Contract No. BRE-CT03-0569.

APPENDIX A: SPIN-POLARIZED THERMIONIC EMISSION

When considering the spin polarization of thermionic emission, we first have to discuss the process of thermionic emission in more detail. Thermionic emission over a barrier of height Φ is generally expressed as[25]

$$J_s = A^{**}T^2\exp(-\beta\Phi), \tag{A1}$$

which applies when the carriers are emitted from a reservoir with an occupation described by a Fermi-Dirac distribution function. The amount of carriers that have enough energy to be emitted over the barrier decays exponentially with barrier height and is strongly reduced at lower temperatures where the distribution function approaches a step function at the Fermi level.

The barrier height Φ is given by the energy difference of the barrier maximum with respect to the Fermi level. In our case of hole emission over the band-bending region of p-type GaAs, the barrier maximum is given by the position of the valence-band maximum at the semiconductor surface. For the current J_{bs} due to emission of holes from the bulk of the semiconductor to the surface, the Fermi level in the semiconductor bulk is relevant. For the current J_{sb} from surface to bulk, the Fermi level at the semiconductor surface should be used. When no voltage across the Schottky barrier is present, the Fermi levels on each side of the barrier are lined up. Carriers on both sides then ''see'' an equal barrier height Φ and the currents J_{bs} and J_{sb} exactly balance each other. The net current is then zero. In the case where a voltage difference is present, carriers on one side will see a lower barrier and $J_{bs}\neq J_{sb}$. The barrier height for emission from bulk to surface is given by $V_{bb}+\xi$, where V_{bb} is the band bending and ξ denotes the difference between Fermi level and valence-band maximum in the bulk. For emission from surface to bulk the barrier height is $V_{bb}+\xi+V_s$. We thus have

$$J_{bs} = A^{**}T^2\exp[-\beta(V_{bb}+\xi)],$$

$$J_{sb} = A^{**}T^2\exp[-\beta(V_{bb}+\xi+V_s)]. \tag{A2}$$

The total current is then given by $J_{sb}-J_{bs}$, which reduces to Eq. (6).

The spin dependence of thermionic emission comes entirely from the spin dependence of the Fermi levels on both sides of the barrier. As already noted, no spin dependence is introduced via the position of the valence-band maximum, as this is determined by electrostatics for which only charge, not spin, is of importance. If we moreover neglect the polarization of valence-band holes in the semiconductor bulk, then the current J_{bs} is independent of spin and for both spin directions given by

$$J_{bs}^{\sigma} = \frac{1}{2}A^{**}T^2\exp[-\beta(V_{bb}+\xi)]. \tag{A3}$$

The factor 1/2 is introduced to account for the two spin directions. The only spin dependence that remains is that of the Fermi levels at the semiconductor surface. With the spin-dependent surface potential V_s^{σ}, the thermionic emission current from surface to bulk becomes

$$J_{sb}^{\sigma} = \frac{1}{2}A^{**}T^2\exp[-\beta(V_{bb}+\xi+V_s^{\sigma})]. \tag{A4}$$

For each spin, the net current $J_{sb}^{\sigma}-J_{bs}^{\sigma}$ can then be written as Eq. (11).

APPENDIX B: SPIN-POLARIZED DIFFUSION PHOTOCURRENT

To evaluate the spin dependence of the diffusive component of the photocurrent, we solve the one-dimensional diffusion equation for both spin orientations. Denoting the excess density of spin-up and spin-down electrons in a steady state by $\Delta n^{\uparrow}$ and $\Delta n^{\downarrow}$, respectively, the diffusion equations read[2]

$$\frac{\delta\Delta n^{\uparrow}}{\delta t} = D\frac{\delta^2\Delta n^{\uparrow}}{\delta x^2} - \frac{\Delta n^{\uparrow}}{\tau} - \frac{1}{2}\frac{\Delta n^{\uparrow}-\Delta n^{\downarrow}}{\tau_s} + R^{\uparrow} = 0,$$

$$\frac{\delta\Delta n^{\downarrow}}{\delta t} = D\frac{\delta^2\Delta n^{\downarrow}}{\delta x^2} - \frac{\Delta n^{\downarrow}}{\tau} - \frac{1}{2}\frac{\Delta n^{\downarrow}-\Delta n^{\uparrow}}{\tau_s} + R^{\downarrow} = 0. \tag{B1}$$

Here $\delta/\delta t$ and $\delta/\delta x$ denote the partial derivative with respect to time t and distance x from the semiconductor surface, respectively, while $R^{\sigma}=C^{\sigma}(f_p/e)\alpha\exp(-\alpha x)$ is the rate of generation of electrons with spin σ. Defining $n^{+}=\Delta n^{\uparrow}+\Delta n^{\downarrow}$ and $n^{-}=\Delta n^{\uparrow}-\Delta n^{\downarrow}$, we can rewrite Eq. (B1) by adding and subtracting the two equations

$$D\frac{\delta^2 n^{+}}{\delta x^2} - \frac{n^{+}}{\tau} + R^{+} = 0,$$

$$D\frac{\delta^2 n^{-}}{\delta x^2} - \frac{n^{-}}{T} + R^{-} = 0, \tag{B2}$$

with $R^{+}=R^{\uparrow}+R^{\downarrow}$, $R^{-}=R^{\uparrow}-R^{\downarrow}$, and $T=\tau/(1+\tau/\tau_s)$. Just as for the non-spin-polarized case,[31] we will impose the boundary conditions $n^{+}=n^{-}=0$ at $x=\infty$ and $x=w$. The first condition is equivalent to assuming that all the light is

absorbed in the semiconductor. The second condition states that the excess density at the edge of the depletion region can be neglected, thus assuming that every photoexcited electron at $x=w$ is immediately swept into the depletion region. The solutions of Eq. (B2) are then given by

$$n^{+}=(C^{\uparrow}+C^{\downarrow})\frac{f_p}{eD}\frac{\alpha L_d^2}{\alpha^2 L_d^2+1}\times\left\{\exp\left(-\alpha w-\frac{x-w}{L_d}\right)-\exp(-\alpha x)\right\},$$

$$n^{-}=(C^{\uparrow}-C^{\downarrow})\frac{f_p}{eD}\frac{\alpha L_s^2}{\alpha^2 L_s^2+1}\times\left\{\exp\left(-\alpha w-\frac{x-w}{L_s}\right)-\exp(-\alpha x)\right\}, \quad \text{(B3)}$$

where $L_d=\sqrt{D\tau}$ is the diffusion length and $L_s=\sqrt{DT}=\sqrt{D\tau/(1+\tau/\tau_s)}$ is the ''spin-asymmetry'' diffusion length. The currents from bulk into depletion region, associated with n^{+} and n^{-}, are obtained from

$$J^{\pm}=eD\left.\frac{dn^{\pm}}{dx}\right|_{x=w}. \quad \text{(B4)}$$

The diffusion photocurrents are then obtained by substituting Eqs. (B3) into Eq. (B4), which yields

$$J^{+}=(C^{\uparrow}+C^{\downarrow})f_p\exp(-\alpha w)\frac{\alpha L_d}{\alpha L_d+1},$$

$$J^{-}=(C^{\uparrow}-C^{\downarrow})f_p\exp(-\alpha w)\frac{\alpha L_s}{\alpha L_s+1}. \quad \text{(B5)}$$

The diffusion photocurrent polarization P_{dif} is then given by J^{-}/J^{+} or

$$P_{dif}=\left(\frac{C^{\uparrow}-C^{\downarrow}}{C^{\uparrow}+C^{\downarrow}}\right)\left(\frac{\alpha+1/L_d}{\alpha+1/L_s}\right). \quad \text{(B6)}$$

To obtain expressions for the spin-up and spin-down diffusive current, we use the relations $J_{dif}^{\uparrow}=(J^{+}+J^{-})/2$ and $J_{dif}^{\downarrow}=(J^{+}-J^{-})/2$. The diffusion photocurrent J_{dif}^{σ} for spin σ is then explicitly written as

$$J_{dif}^{\sigma}=\frac{1}{2}f_p\exp(-\alpha w)\left\{\frac{\alpha L_d}{\alpha L_d+1}\pm\frac{\alpha L_s}{\alpha L_s+1}(C^{\uparrow}-C^{\downarrow})\right\}, \quad \text{(B7)}$$

where the plus sign should be used for $\sigma=\uparrow$ and the minus sign for $\sigma=\downarrow$. We then have Eq. (16). Note that we have used $C^{\uparrow}+C^{\downarrow}=1$.

*Present address: Francis Bitter Magnet Laboratory, Massachusetts Institute of Technology, Cambridge, MA 02139.

†Present address: Philips Research Laboratories, Prof. Holstlaan 4, 5656 AA Eindhoven, The Netherlands.

[1] *Optical Orientation*, edited by F. Meier and B. P. Zakharchenya, Modern Problems in Condensed Matter Sciences Vol. 8 (Elsevier, Amsterdam, 1984).

[2] D. T. Pierce, R. J. Celotta, G.-C. Wang, W. N. Unertl, A. Galejs, C. E. Kuyat, and S. R. Mielczarek, Rev. Sci. Instrum. **51**, 478 (1980).

[3] F. Ciccacci, E. Vescovo, G. Chiaia, S. De Rossi, and M. Tosca, Rev. Sci. Instrum. **63**, 3333 (1992).

[4] W. T. M. Wolters, Master's thesis, University of Nijmegen, 1988.

[5] D. T. Pierce, Phys. Scr. **38**, 291 (1988).

[6] M. W. J. Prins, D. L. Abraham, and H. van Kempen, J. Magn. Magn. Mater. **121**, 109 (1993); Surf. Sci. **287/288**, 750 (1993).

[7] M. W. J. Prins, H. van Kempen, H. van Leuken, R. A. de Groot, W. Van Roy, and J. De Boeck, J. Phys.: Condens. Matter **7**, 9447 (1995).

[8] M. W. J. Prins, M. C. M. M. van der Wielen, R. Jansen, D. L. Abraham, and H. van Kempen, Appl. Phys. Lett. **64**, 1207 (1994).

[9] R. Jansen, M. C. M. M. van der Wielen, M. W. J. Prins, D. L. Abraham, and H. van Kempen, J. Vac. Sci. Technol. B **12**, 2133 (1994).

[10] S. N. Molotkov, Pis'ma Zh. Éksp. Teor. Fiz. **55**, 180 (1992) [JETP Lett. **55**, 173 (1992)].

[11] R. Laiho and H. J. Reittu, Surf. Sci. **289**, 363 (1993).

[12] J. H. Reittu, J. Phys.: Condens. Matter **6**, 1847 (1994).

[13] M. W. J. Prins, R. Jansen, R. H. M. Groeneveld, A. P. van Gelder, and H. van Kempen, Phys. Rev. B **53**, 8090 (1996).

[14] An early version of the model was already published in Ref. 15.

[15] M. W. J. Prins, R. Jansen, and H. van Kempen, Phys. Rev. B **53**, 8105 (1996).

[16] Note that this matrix element is not the same as the one introduced by Bardeen in Ref. 17, but rather a pseudo matrix element as used by Feuchtwang (Ref. 18). This allows the description of the tunnel current in terms of the densities of states.

[17] J. Bardeen, Phys. Rev. Lett. **6**, 57 (1961).

[18] T. E. Feuchtwang, Phys. Rev. **13**, 517 (1976).

[19] R. K. Ahrenkiel, in *Minority Carriers in III-V Semiconductors: Physics and Applications*, edited by R. K. Ahrenkiel and M. S. Lundstrom, Semiconductors and Semimetals Vol. 39 (Academic Press, San Diego, 1993), Chap. 2, p. 39.

[20] C. J. Chen, *Introduction to Scanning Tunneling Microscopy*, Oxford Series in Optical and Imaging Sciences Vol. 4 (Oxford University Press, New York, 1993).

[21] This is only immediately evident from Eq. (4) when the spin-integrated term equals zero. This happens when $\Delta V_s^{\uparrow}=-\Delta V_s^{\downarrow}$, i.e., when the optical modulations of the surface potential of the two spin orientations have equal magnitude but are out of phase. As will be shown in Sec. II B, this is not generally true because tunneling into the ferromagnet can influence the surface potentials V_s^{σ}. However, even in this case a simple symmetry argument, based on the reversal of the spin-quantization axis, shows that the *sum* of the spin-integrated and spin-selective terms in Eq. (4) should change sign upon magnetization reversal.

[22] M. W. J. Prins and A. P. van Gelder, Physica B **218**, 297 (1996).

[23] The definitions of Φ_s and ξ are such that they have a negative sign for the case of a *p*-type semiconductor under consideration here. Both parameters are defined in volts.

[24] M. S. Sze, *Physics of Semiconductor Devices* (Wiley, New York, 1981).

[25] E. H. Rhoderick and R. H. Williams, *Metal-Semiconductor Con-*

tacts, Monographs in Electrical and Electronic Engineering No. 19 (Clarendon, Oxford, 1988).

[26] H. K. Henisch, *Semiconductor Contacts*, International Series of Monographs on Physics No. 70 (Clarendon, Oxford, 1984).

[27] R. Maboudian, K. Pond, V. Bressler-Hill, M. Wassermeier, P. M. Petroff, G. A. D. Briggs, and W. H. Weinberg, Surf. Sci. Lett. **275**, L662 (1992).

[28] For the case that the density of surface states equals zero, the exact barrier height is calculated by W. J. Kaiser, L. D. Bell, M. H. Hecht, and F. J. Grunthaner, J. Vac. Sci. Technol. A **6**, 519 (1988).

[29] Z.-H. Huang, M. Weimer, and R. E. Allen, Phys. Rev. B **48**, 15 068 (1993).

[30] In principle, this statement is only valid in the case where the level occupation follows a Fermi-Dirac distribution function. Deviations from thermal equilibrium may produce an additional spin dependence.

[31] C. M. Aldao, A. Palermo, and J. H. Weaver, J. Vac. Sci. Technol. A **10**, 493 (1992).

[32] In the context of spin-polarized electron sources, photocurrent is usually described as a three-step process, the third step being the escape of the photoelectrons from the semiconductor into the vacuum. In our case of a tunneling junction, this third step is replaced by tunneling or recombination with a thermionically emitted valence-band hole. These two current paths are treated separately in our model and in the present discussion, photocurrent only refers to the first two steps.

[33] K. Zerrouati, F. Fabre, G. Bacquet, J. Bandet, J. Frandon, G. Lampel, and D. Paget, Phys. Rev. B **37**, 1334 (1988).

[34] T. Murayama, R. Prepost, E. L. Garwin, C. K. Sinclair, B. Dunham, and S. Kalem, Appl. Phys. Lett. **55**, 1686 (1988).

[35] The division by 2 is necessary because D_{ss} is the spin-integrated density of surface states.

[36] For vanishing D_{ss} the modulation given by Eq. (20) becomes infinite; however, the model does not apply to this limit.

[37] Omitting capacitances has only a minor influence on the CPM signal. To illustrate this we note that according to Ref. 13, the modulation signal is proportional to $Y_t/(Y_t+Y_s)$. Here $Y_t=\tilde{G}_t+j\omega\tilde{C}_t$ and $Y_s=\tilde{G}_s+j\omega\tilde{C}_s$ are the complex admittances of the tunnel and Schottky barrier, respectively, defined per unit area. Using $\tilde{C}_s=\epsilon_0\epsilon_s/w$, $\epsilon_s=12.9$, and $w\approx 30$ nm, we have $\tilde{C}_s\approx 3\times 10^{-3}$ F m^{-2}. Similarly, $\tilde{C}_t=\epsilon_0/d$, where $d\approx 1$ nm is the width of the tunnel barrier. This gives $\tilde{C}_t\approx 10^{-2}$ F m^{-2}. In our calculations we have used $\tilde{G}_t>10^6$ Ω^{-1} m^{-2}, while the conductance $\tilde{G}_s$ through the Schottky barrier varies from a few times 10^6 Ω^{-1} m^{-2} at forward bias to 10^3 Ω^{-1} m^{-2} at reverse bias. For a typical modulation frequency of, say, 10 kHz used in experiments, we can easily see that neglecting the capacitances produces an error smaller than 10^{-6} in the magnitude of $Y_t/(Y_t+Y_s)$. This can safely be neglected.

[38] R. Jansen, Ph.D. thesis, University of Nijmegen, 1997.

[39] R. Meservey and P. M. Tedrow, Phys. Rep. **238**, 173 (1994).

[40] Strictly speaking, the ratio τ/τ_s of minority carrier lifetime and spin lifetime is the relevant quantity determining depolarization. In our calculations we have treated τ as a constant and varied only τ_s.

[41] M. W. J. Prins, R. H. M. Groeneveld, D. L. Abraham, H. van Kempen, and H. W. van Kesteren, Appl. Phys. Lett. **66**, 1141 (1995).

[42] H.-J. Drouhin, C. Hermann, and G. Lampel, Phys. Rev. B **31**, 3872 (1985).

[43] F. Meier, D. Pescia, and M. Baumberger, Phys. Rev. Lett. **49**, 747 (1982).

[44] F. Meier, G. L. Bona, and S. Hüfner, Phys. Rev. Lett. **52**, 1152 (1984).

[45] F. Meier, in *Polarized Electrons in Surface Physics*, edited by R. Feder (World Scientific, Singapore, 1985).

[46] R. Allenspach, F. Meier, and D. Pescia, Appl. Phys. Lett. **44**, 1107 (1984).